Renewable Energy 136 (2019) 1255–1265

Contents lists available at ScienceDirect

Renewable Energy

journal homepage: www.elsevier.com/locate/renene

Chaotic dynamics applied in time prediction of photovoltaic production

Hasnaa Bazine*, Mustapha Mabrouki

Industrial Engineering Laboratory, Faculty of Science and Technology, Sultan Moulay Slimane University, B.P: 523, Beni Mellal, Morocco

ARTICLE INFO

Article history:
Received 5 July 2018
Received in revised form
12 September 2018
Accepted 27 September 2018
Available online 29 September 2018

Keywords:
Chaotic time series
Phase space reconstruction
Second generation wavelets
Recurrent neural network (RNN)
Renewable energy forecasting
Power planning

ABSTRACT

The advantage of accurate forecasts is that it solves the main problem related to renewable energies: their variability. Indeed, while renewable energies has not yet replaced fossil fuels, in spite of the efforts of many governments, it is because of their intermittent nature, hence the importance of prediction in this field. The new approach for energy prediction that we propose in this paper, is founded on the analysis of the dynamical behavior of the photovoltaic production of the Faculty of Sciences and Technology of Beni Mellal, Morocco. It consists in performing the phase space reconstruction, which allowed us later to build a database for the input of the neural network and thus take into account the dynamics of the system in the forecasting process. Then, in search of more precision, we introduce the wavelet transformation, to simplify the database constructed from phase space reconstruction. Finally, comparing between the predictions and the actual observations confirmed the efficiency of our approach.

1. Introduction

Determined differential equations can describe the temporal evolution of many natural phenomena. Solving these must allow us to find what happens to the system over time However, there are a number of systems that cannot be modeled, and even if a mathematical model exists, to resolve it is often complicated, if not impossible. Thus, the predictability of the future state of these systems is now an endless quest.

Fig. 1 shows the daily evolution of photovoltaic production at the Faculty of Science and Technology of Beni Mellal between 01/01/2015 and 21/12/2016. We cannot fail to notice its extreme irregularity. We notice irregular fluctuations that never occur identically. A direct consequence of aperiodicity in the curve of photovoltaic production is the great difficulty of the forecast. Unlike the periodic and quasi-periodic phenomena for which a long-term forecast is possible, as has been demonstrated for a long time by the impressive successes of astronomy, the forecast in the case of renewable production and particularly that of photovoltaics is very limited in time. The remarkable progress made over the past decades, in particular following the use of powerful computers, have achieved reliable forecasts up to several days of maturity. However, all the experiments show that the success decreases with the duration of the forecasts, and that beyond a number of days, the daily forecasts become random, because of the growth of uncertainties.

Faced with these findings, It is normal to wonder if this lack of reliability is the consequence of the imperfection of our current models. Or if is there a more fundamental reason that limits the possibility of predicting beyond a certain period.

A first answer that comes to mind is to attribute these difficulties to the extreme complication of the atmospheric or climatic environment, which encompasses many factors, ranging from temperature, precipitation, humidity, to wind speed. In this perspective, the difficulties related to forecasting would be a temporary inconvenience, doomed to disappear as the parameters are accessible by advanced observation techniques, and computers that we have available will become more efficient allowing thus a resolution that is growing in accuracy.

However, there is another possibility that may explain the aperiodic nature and limited predictability of photovoltaic production, which is to be found in the “complexity” of the subjacent non-linear dynamics. The physical and mathematical sciences suggest a prototype able to give birth to such complexity: the deterministic chaos whose most characteristic signature is the phenomenon of initial conditions sensitivity.

* Corresponding author.
E-mail address: hasnaa.bazine@gmail.com (H. Bazine).

https://doi.org/10.1016/j.renene.2018.09.098
0960-1481/

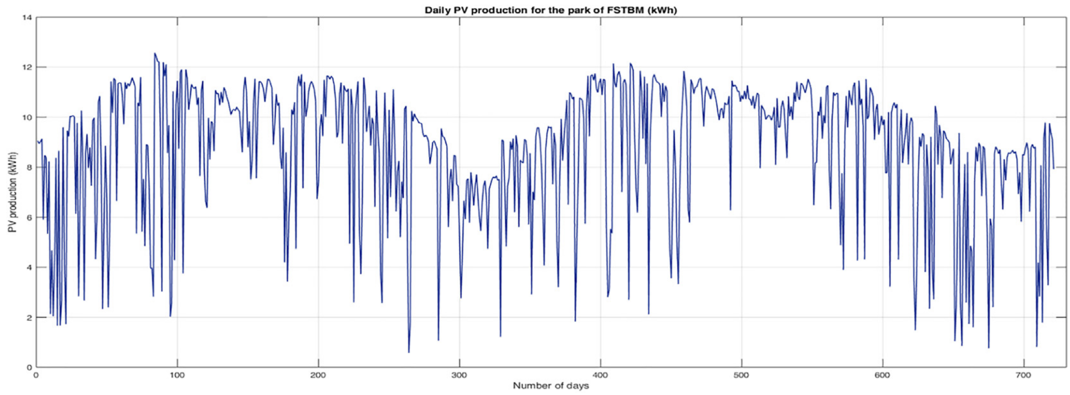

Fig. 1. Daily evolution of photovoltaic production at the Faculty of Science and Technology of Beni Mellal.

In this sense, we can divide dynamic systems into three types: random systems (also called stochastic systems), deterministic systems and chaotic systems. Random systems evolve, as their name suggests, randomly in all space, without any equation regulating them, without any possible and exact prediction over time. Deterministic systems are systems governed by well-known mathematical laws, so we can predict exactly the evolution of these systems over time. Chaotic systems, in contrast, have an infinitely complex behavior. They are irresistibly attracted by a geometric figure of structure also infinitely complex on which they seem to wander at random, but never leave it, or go back twice by the same point. The attractors that characterize these systems seem to include both deterministic and random laws.

The birth of the theory of chaos began when Henri Poincare, one of the famous mathematicians of our time and certainly the most universal, decided to take up the challenge of King Oscar in 1889. It is about solving the problem of the behavior of three planets, which could be summarized as follows: "Is the solar system stable?" Poincare soon discovered that the solutions of Newton's equations were nonintegrable in the case of three planets. He had the brilliant idea of approaching the problem in another way, by geometry. He made-up the concept of phase space, and concludes that the trajectories of three interacting planets were unpredictable. The solar system did not work like a clock. For the first time, Newton's laws showed their limits, and the future proved unpredictable. More recent researches have confirmed that the solar system was really unstable and chaotic. Disturbances are multiplied by 10^{10}, or ten billion, in one hundred million years [1].

However, since he did not possess a computer, Poincare could not go beyond his reasoning and simulate the behavior of the three planets in their phase space, as did later Edward Lorenz, who would have discovered the strange attractors and chaos. His famous article in 1963 [2], marked the official birth of the theory of chaos. By demonstrating through the numerical resolution of a system representing a cellular convection that the solutions found and which were non-periodic, are usually unstable compared to small modifications, so that a slight difference in the initial state can evolve to a considerable difference in final state. The possibility of realizing very long-term weather predictions is examined in view of these results.

Recently, the study of chaotic dynamics, initially limited to pure mathematics, has literally invaded the physical sciences. The mathematician and meteorologist, E. Lorenz when he proposed, in 1963, one of the first examples of this type of model, which generates a chaotic behavior from a physical problem, played the pioneering role in this area. Chaotic behavior has been observed since then, in very diverse systems studied, in astronomy [3], climatology [4], chemistry [5], fluid dynamics [6], biology [7], as well as in medicine [8], economics [9,10], mechanical [11–13] and electrical applications [14,15], and even in the topography [16] and explanation of natural phenomena [17,18]. The spectacular development of this "new" dynamic has given birth to concepts and methods for describing, classifying and modeling these behaviors in a unified way.

Several variables such as temperature, wind speed or humidity … influence the state of a physical system such as the photovoltaic station, at different points of space. These variables change according to laws which are in the form of nonlinear differential equations in the sense that the variables are involved in a way that deviates significantly from a simple proportional relation. We know that in the presence of nonlinearities any attempt at a complete quantitative solution of the equations is doomed to failure. Therefore, it is essential to set up qualitative methods of analysis.

The objective in this work was to perform a chaotic analysis to ameliorate predictions made with artificial intelligence tools. As a prediction tool we have chosen to use neural networks, which, despite their effectiveness, are often seen as being black box solutions. But on the other hand, they may provide very useful results. However, they remain a very interesting topic for researchers who wish to improve the performance of these networks and extend their scope of applications. Thus, to emphasize the significance of the analysis of the non-linear dynamics of complex systems, we developed the predictions without and with the phase space reconstruction and then compare the performance in both cases. Then we used the wavelet transform upstream of the neural network, to further improve the precision of the predictions.

2. Material and method

The initial idea is to detect the existence of chaos in the dynamics of our system. To do this we have chosen to apply two methods to compare the results. In the first method, it is a question of calculating the exponent of Lyapunov, as for the second, it is called the 0–1 test. The next step was dedicated to the phase space reconstruction, to visualize the state evolution of the system over time. The most important technique for phase space reconstruction is Takens' theorem, also called the delay method. The reconstruction of the phase space will allow us later to build the database for the neural network input is and so integrate the system dynamics in the forecasting operation.

2.1. Data and study site

The studied site is the photovoltaic park of the Faculty of

Sciences and Technologies of Beni Mellal, of which we will exploit the history of production like time series. This time series include 721 values from 01/01/2015 to 21/12/2016.

Fixed on the roof of the research center, the PV system considered in this work has a total area of approximately 1570 m^2. Its modules are made of amorphous silicon and oriented towards S. The fixed PV panels were mounted on the S roof of the building with 30° of inclination. With the absence of buildings in the vicinity that can cast shadows on photovoltaic panels. . A measurement and analysis program monitors the output by performing data acquisition in PV inverter systems. The university can use directly the PV power generation. The PV power generation can be directly used by the university since the inverters are connected to the 220 V three-phase circuit in parallel with the national provider electrical grid.

2.2. Chaos detection

2.2.1. Largest Lyapunov exponent

The most popular approach for quantifying the presence of chaos in dynamical systems is to examine the property of initial conditions sensitivity by means of Lyapunov exponents [19,20].

The exponent of Lyapunov measures the divergence of the trajectories from points that were initially very close, thus indicating the degradation of predictability over time. The Lyapunov exponent quantifies initial conditions sensitivity. Moreover, the sign of the Lyapunov exponents allows the classification of attractors. A negative Lyapunov exponent indicates a tightening of the trajectories on the attractor, which means the absence of sensitivity to the initial conditions, whereas a positive Lyapunov exponent denotes on the contrary the divergence of the trajectories on the attractor and thereafter the initial conditions sensitivity.

Let $Z : X \to X$ be a map in general setting (not necessarily differentiable), and$X \subseteq R^d$. For every point x in the interior of X, and for every y in R^d, the local Lyapunov exponent of Z at x with respect to direction y is defined as the limit (if it exists)

$$\lim_{\delta\to 0}\ln\frac{\|Z(x+\delta y)-Z(x)\|}{\|\delta y\|} \tag{1}$$

The global Lyapunov exponent of Z at x with respect to y is defined as the limit (if it exists)

$$\lim_{t\to\infty}\frac{1}{t}\lim_{\delta\to 0}\ln\frac{\|Z^t(x+\delta y)-Z^t(x)\|}{\|\delta y\|} \tag{2}$$

If the global Lyapunov exponent of Z at x with respect to y equals λ then, for all sufficiently large values of t for all small enough values of δ (with respect to the value of t), we have

$$\frac{\|Z^t(x+\delta y)-Z^t(x)\|}{\|\delta y\|}\approx e^{\lambda t} \tag{3}$$

If λ is positive, then we will have an exponential divergence of neighboring trajectories and consequently of chaos. There are various algorithms for estimating the largest exponent of Lyapunov from the time series observation. Taking into account the small size of our sample, we chose to work with the Rosenstein algorithm [2].

2.2.2. The 0–1 test

In this step, we used the 0–1 test to define the nature of our system, in other words, to distinguish between the regular dynamics, that is to say periodic or quasi-periodic, and the chaotic dynamics in our study case.

An important challenge in dynamic systems is the understanding of the internal dynamics of a non-linear system, given only the observed results. Most often, we observe (in numerical or experimental work) a time series regularly spaced by one or more variables, and for several decades, the field of analysis of nonlinear time series has tried to produce means of characterizing complex time series, and especially to differentiate the deterministic chaotic dynamics of small dimension from the stochastic movement. Most diagnostic tools, such as estimating Lyapunov exponents, require large amounts of data, noiselessly, to perform well. Recently, Gottwald & Melbourne have proposed a much simpler test for the presence of deterministic chaos [21]. Their "0–1 test for chaos" uses directly the time series of measurements as input without involving any data pretreatment and returns a single scalar value usually in the range [0,1]. Theoretically, in the case of an infinite quantity of data without noise, the test returns the value 1 in the presence of a deterministic chaos and 0 in the opposite case.

Let X(n) be a one-dimensional time series that we will take as input of the test with n = 1,2 … the data X(n) is used to drive the following 2-dimensional system:

$$\begin{aligned} p(n+1) &= p(n) + X(n)\cos cn, \\ q(n+1) &= q(n) + X(n)\sin cn, \end{aligned} \tag{4}$$

Where $c \in (0, 2p)$ is fixed.

The (time-averaged) mean square displacement is defined by:

$$M(n) = \lim_{x\to\infty}\frac{1}{N}\sum_{j=1}^{N}\left([p(j+n)-p(j)]^2+[q(j+n)-q(j)]^2\right),\ n = 1,2,\ldots \tag{5}$$

And its growth rate is written:

$$K = \lim_{n\to\infty}\frac{\log M(n)}{\log n} \tag{6}$$

We can show, under the general conditions that the limits M (n) and K exist, and K is either equal to 0 meaning regular dynamic, or equal to 1 in the case of a chaotic dynamic.

2.3. Phase space reconstruction

The initial idea of quantitative analysis is to represent the evolution in phase space. The phase space is an abstract multidimensional space subtended by the set of variables describing the system evolution. In this space, a point represents an instantaneous system state an instantaneous system state is represented by a point, and as time passes, the point in question describes a curve, that we call the phase trajectory. By following trajectories that emanate from different initial states, we will obtain what we call a "phase portrait" that will provide a qualitative idea that describes the behavior of the system very well. In most systems we know, after a while the trajectory of the phases will converge towards an object of dimension strictly smaller than that of the phase space, it's called an attractor.

2.3.1. Takens' theorem

Suppose that x_t is a time series generated by an unknown process, with $= 1, \ldots\ldots N$. In order to understand the underlying dynamics of the system, we are limited ourselves to the study of the dynamics on the attractor and from the initial series x_t we can also generate different signals. As such, we will seek to reconstruct the system attractor from the observed time series. For this, we form $(N-m+1)$ vectors at m Dimensions, $\{x_t^m\}_{t=1,\ \ldots,N-m+1}$ called m-historical, whose components are the consecutive values of the observed series shifted by a delay or fixed delay τ:

$$x_t^m = \left(x_t, x_{t+\tau}, x_{t+2\tau}, \ldots, x_{t+(m-1)\tau}\right) \tag{7}$$

With $t = 1, \ldots, N - m + 1$, where the embedding dimension noted m, is the phase space dimension in which the attractor is reconstructed. Takens' theorem establishes that on condition of choosing m large enough, the behavior of the m-histories will mimic that of the underlying dynamic system unknown. In particular, if the dynamics of the system present a chaotic behavior, the m-histories will also have a chaotic behavior. In practice, if $m \geq 2n + 1$, where n is the unknown dimension of the state vector. The attractor thus reconstructed, will have identical topological properties as the initial system. Several techniques were explored in order to choose the delay and the optimal embedding dimension [3,4].

If the phase space is represented in three dimensions, this series of points can graphically exhibit the system evolution over time. The whole possible trajectories constitute the phase portrait. This can help to perceive the attractor of the system.

2.3.2. Choice of time delay

The choice of delay is essential in Taken's theorem. For small delays, restricted resolutions cause an intersection of trajectories that seems to violate causality. A delay time, which is larger than the characteristic recurrence time T, of the system shows causes the coordinates to disjoin by stretching and folding. The embedding space is well utilized, but one observes an "overfolding" of the attractor. For the choice of time delay or lag τ, different intuitive methods have been used.

2.3.2.1. Autocorrelation function. The first zero of the autocorrelation function, for example, guarantees independence between $x(t)$ and$x(t+\tau)$.

Let $X = \{X_1, \ldots, X_n\}$ a discrete time process. The correlation (or autocorrelation) function of X is given by:

$$\varphi(t, t+\tau) = \frac{E[X_t X_{t+\tau}] - E[X_t]E[X_{t+\tau}]}{Var(X_t)Var(X_{t+h})} \tag{8}$$

In general; we use autocorrelation to characterize linear dependencies in residual series (ie time series corrected for trend and season) [23]. Indeed, trend and season are deterministic components and it makes little sense to estimate statistical properties of deterministic quantities. Moreover, if the series studied have their characteristics evolving over time. Their statistical properties can be hard to estimate, because generally we have only one realization of the process that is insufficient to the estimation.

2.3.2.2. First minimum of mutual information. The mutual information function can nevertheless guarantee more general independence, which represents the dependence degree of two variables in the probabilistic sense. It is defined by the sum that links density of probability to marginal distributions:

$$I(X,Y) = \int_{\mathbb{R}}\int_{\mathbb{R}} p(x,y) Log \frac{p(x,y)}{p(x)p(y)} dxdy \tag{9}$$

Where $p(x,y)$, $p(x)$ and $p(y)$ are respectively the densities of the laws of(X,Y), X and Y.

On a time series, the mutual information estimates the predictability degrees of the future samples of the time series from the previous samples. It's considered the non-linear version of autocorrelation. We use the mutual information to calculate the delay τ in calculating the phase space of a time series. This measures the predictability degrees of $x(t+\tau)$ from$x(t)$. In the reconstructing phase space process, the delay method is to choose a parameterτ, which separates values so that they are relatively independent of each other, while being sufficiently correlated with the output. It's a kind of compromise between redundancy and relevance. Thus we calculate the mutual information between two variables $x(t)$ and $x(t+\tau)$ for increasing values ofτ. The criterion used is to take the time that corresponds to the first local minimum (τmin) of mutual information.

2.3.3. Choice of embedding dimension

To define the optimal embedding dimension, we used the nearest false neighbors algorithm [22,24]. The principle of this algorithm is that when an object in dimension m is projected in lower dimension, some initially distant points become neighbors. We are talking about false neighbors. Conversely, starting from dimension 1, the number of false neighbors at each passage to the next dimension should decrease until it becomes zero when the topology of the attractor is fully revealed.

2.4. Prediction

In our approach, the reconstruction of the phase space will allow us to build the database that will be the input of the neural network for the prediction. The idea here is to provide the neural network with a full and sufficient description of the system by the phase space reconstruction. We will then compare the prediction with and without phase space reconstruction to emphasize the advantage of such an analysis. Then we will insert the Discrete Wavelet Transformation DWT to simplify the database built from the reconstruction of the phase space before transmitting it to the neural network to perform the prediction for more accuracy.

To develop this work, we used Matlab 2015a from MathWorks, the US software company specializing in mathematical calculation software. We have also exploited the Wavelet Toolbox to make the Discrete Wavelet Transform DWT, and the neural network Toolbox in the objective to use past values of our time series to forecast the future ones using a multilayer network.

2.4.1. Artificial neural networks

Several works use the Artificial neural networks (ANNs) for prediction in the case of chaotic time series [25]. Neurons are connected processing units to form an ANN. These networks are inspired by the humans' cognitive process. And have a great success in prediction and especially in the field of renewable energies, as prediction of solar energy generation [26–28], wind power generation [29], wind speed [30], solar irradiance [31]. One of the advantages of an ANN is experimental learning. The relative speed with which ANNs perform the calculations and their robustness are other advantages of neural networks.

In artificial intelligence, the ANN models are simple mathematical models that define a function $f: X \rightarrow Y$ or distribution defined on X or on X and$Y$.

Mathematically, the function$f(x)$ of the artificial neural network is defined as a composition of other functions$g_i(x)$. ANN is usually represented as a network structure, where arrows represent dependencies between variables. In most cases, we use the weighted nonlinear sum, where $f(x) = K\left(\sum_i \omega_i g_i(x)\right)$ with $K$is the activation function (obtained in our case by the DWT). The most important role of the activation function is to provide a smooth transition when changing the input values, so a small input change produces a small variation in the output.

Fig. 2 describes the Mathematical Model of a Nonlinear Neuron.

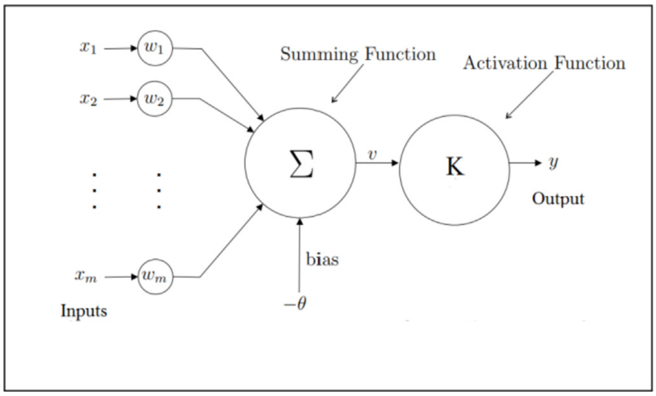

Fig. 2. Mathematical model of a nonlinear neuron.

2.4.2. Recurrent Wavelet Neural Networks (WRNN)

The concept of Recurrent Wavelet Neural Networks (WRNN) is based on the theory of wavelet transform, combined with neural networks, different algorithms based on wavelet network were proposed in literature. The prediction with wavelet neural networks is a topic that has been widely explored, for example The WRNN has been used to forecast energy fluctuation [32], wind power generation [33], solar irradiance [34] or again wind speed [35].

Our WRNN-based predictors use a time series that represents photovoltaic production. We calculate a discrete wavelet decomposition of each time series by performing the multi resolution analysis to obtain the proper input set for the WRNN as required by the designed architecture.

Firstly, it is a question of decomposing our time series in approximation (Ak) and in details (Dk), by using discrete wavelet transformation DWT. After that, we performed a level 3 signal decomposition using The Daubechies wavelets Db1. The final approximation A3 and details (D1, D2, D3) obtained at the 3rd level was used as input for the neural network, with which we made the forecasts to obtain the prediction of the original time series. We divided the set of data randomly into 3 subsets: training, validation, and testing. The training set forms the model, that is, to adjust the model parameters. The validation set is used to reassure that there will be no overfitting in the final results. The performance of the model is evaluated by the test, as it provides an independent measure of how the network can be expected to work on data that has not been used in training. We reserved 70% of data for training, 15% for validation and the 15% that remain for the test.

In multilayer networks, the main problem is to define the hidden layers neurons number, so as to obtain the best accuracy/speed ratio. In fact, too many neurons increase the calculation time excessively, but also give better results (not always). There are currently no reliable methods for finding the optimal configuration. So we tried several configurations of networks to choose the best in both studied cases. The chosen configuration for this case is a single hidden layer network with 16 neurons.

2.4.3. Discrete wavelet transform

Basically, the discrete wavelet multi-resolution analysis, commonly based on Daubechies (db) orthogonal wavelet basis, consists of introducing the signal to be analyzed into a low-pass filter (Lp) and high-pass filter (Hp). At this level, we obtain two vectors: A_1 and D_1. The vector A_1 is composed of approximations, they include low frequencies of the signal, while the elements of the vector D_1 are called details, and they include high frequencies of the signal. We repeat the same operation with the vector A1 and successively with each new vector A_k obtained, until it reaches the number n which is the number of levels. The filters set is called filter bank.

The A_k approximations and details D_k satisfying the relations:

$$A_{k-1} = A_k - D_k \tag{10}$$

$$S = A_k + \sum_{i \le k} D_i \tag{11}$$

With:

S: the original signal
K: the number of decomposition. $1 \le k \le n$

The decomposition for the case of 3 levels, n = 3 is presented in Fig. 3:

2.5. One-dimensional wavelet neural network

The primary wavelet neural networks form is simply a single input and output network. The hidden layer of neurons consists of wavelets whose input parameters include the coefficients of expansion and translation of the wavelets. The hidden layer's wavelets produce a non-zero output when the input is in a small area of the input domain. Then, the wavelet neural network output is the linear weighted combination of wavelet activation functions. It is defined as:

$$\psi_{\tau,s}(t) = \psi\left(\frac{t-\tau}{s}\right) \tag{12}$$

Where τ and s respectively represent the shift and scale parameters.

Fig. 4 shows the architecture of a Basic wavelet network. There is only one input and one output, and the hidden layer consists of M wavelets. The output neuron is a summation function. It generates a weighted sum of the wavelet outputs.

$$y(t) = \sum_{i=1}^{M} \omega_i \psi_{\tau_i,s_i}(t) + \overline{y} \tag{13}$$

In order t deal with functions whose mean is not zero, we add the value$\overline{y}$, considering that the wavelet function is of zero mean. The value $\overline{y}$ is a substitution for the scaling function$\varphi(t)$, at the largest scale, of the wavelet multi-resolution analysis.

In a wavelet network, all parameters$\overline{y}$,ω_i, $s_i$et τ_i are adjustable by training algorithm.

3. Results and discussion

3.1. Lyapunov exponent

The algorithm for calculating the Largest Lyapunov exponent has elapsed at a time of 11.267240 s.

We found a value of 0.3198 which is positive. Therefore we deduce that in our case we have a chaotic system. Fig. 5 shows Lyapunov exponents for various k_s. We notice that the plot of this exponents have smooth part (or fairly horizontal) and that prove that the parameters were selected correctly.

3.2. 0–1 test

For the case of photovoltaic production we found k = 0.997892776665315 which is close to 1. We deduce that we are

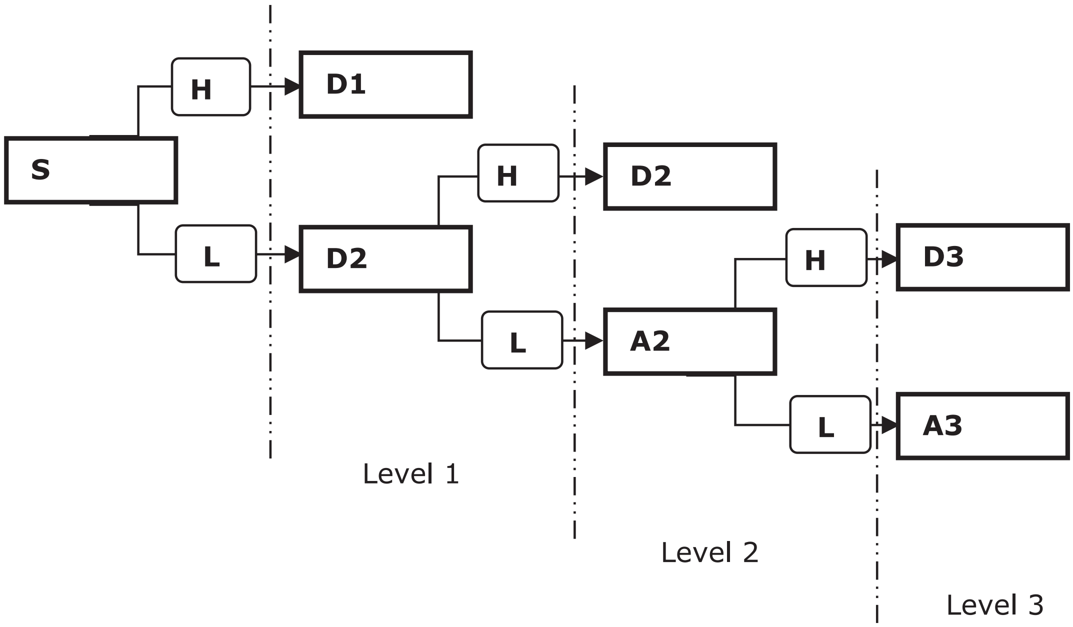

Fig. 3. Three-levels wavelet decomposition.

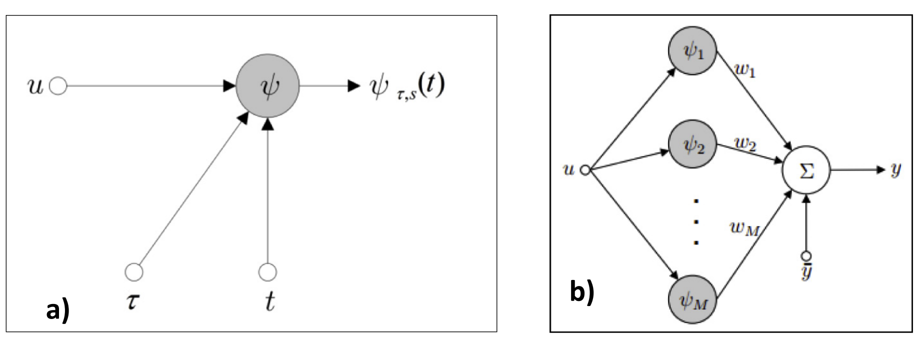

Fig. 4. a) A Wavelet Neuron b) a Wavelet Neuron Network.

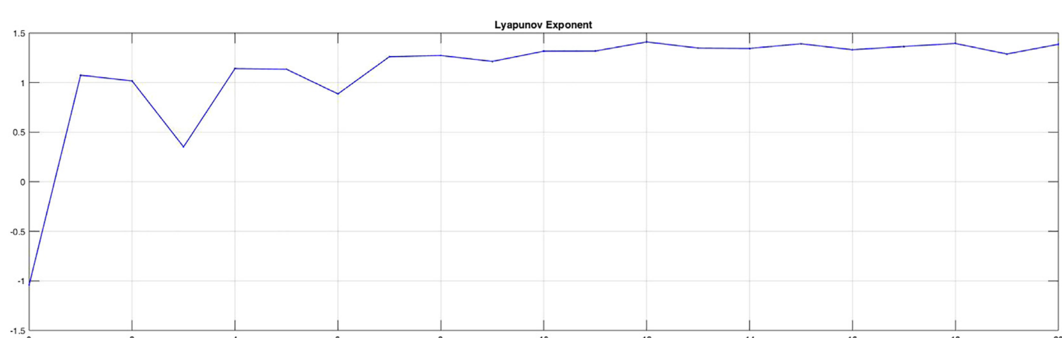

Fig. 5. Lyapunov exponents for various ks.

in the case of chaotic system.

First, the chaotic behaviors are studied in the logistic map by employing the new coordinates of translation variables p(n) and q(n), which are shown in Fig. 6.

We note an asymptotic Brownian motion for underlying chaotic dynamics. For $\mu = 3.97$ (which corresponds to chaotic dynamics), the system exhibits chaotic dynamics.

To analyze the diffusive (or non-diffusive) behavior of pc and qc we compute the mean square displacement $M_c(n)$.

Fig. 7 shows the mean square displacements $M_c(n)$ for the logistic map $x_{n+1} = \mu x_n\ (1-xn)$ with $\mu = 3.97$ (which corresponds to chaotic behavior) with an arbitrary value of $c = 0.9$. The subtraction of the oscillatory term V_{osc} (c,n) regularizes distinctly the linear behavior of $M_c(n)$. This allows us to better determine the mean squared displacement and the asymptotic growth rate K_c, which is presented in the following (see Fig. 8).

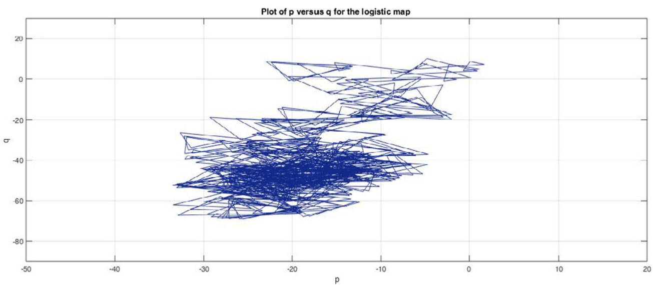

Fig. 6. The translation variable p versus q.

We notice that most values of K_c are very close to 1. Thus, PV time series shows chaotic behavior. Different values of c are chosen to characterize the PV system.

3.3. *The first zero of the autocorrelation function*

For photovoltaic production in our case, we see in Fig. 9, that the first zero of autocorrelation function is obtained for a time lag $\tau = 77$ days.

3.4. *The first minimum of mutual information*

Fig. 10 shows that the mutual information function is minimal for the first time for $\tau = 3$ days.

3.5. *Minimum embedding dimension*

Fig. 11 shows the embedding dimension. Good values are those with a percentage of false neighbors close to zero. The result reveals that the percentage of false neighbors is less than 20% in a space of dimension equal to 4 which is the optimal embedding dimension.

Fig. 12 shows the phase portrait in three dimensions of the attractor reconstructed for the series of photovoltaic daily production.

It is found that the resulting curve signals indicate both the presence of a disorder in the pure state (the points are scattered randomly on the shape obtained) and that of an unsuspected order (the curve describes a precise shape despite his strangeness). These trajectories are tight, without ever really joining, without ever intersecting. However they remain inside a finite space in a cube. It seems that our system behaves in fact as if it were guided by an invisible underlying model, an order, a hidden constraint, a “phase space” towards which all its trajectories converge.

3.6. *Results of the prediction*

For the purpose of forecasting the evolution of photovoltaic production, we used different methods. At first, we only used the neural networks, and then we redid the predictions, but this time using the results of the reconstruction of the phase space to enrich the neural network's input and ameliorate the precision. Finally we introduced the wavelet transformation to simplify the database resulting from the reconstruction of the phase space and which fed the neural network for better results. For all these methods, the mean squared error (MSE) was calculated in the three phases of the forecasting process, namely training, validation and testing, the results of this calculation are exposed in Table 1. Moreover, we calculated the regression coefficients for used methods and in each phase of the process, Table 2 present the obtained results.

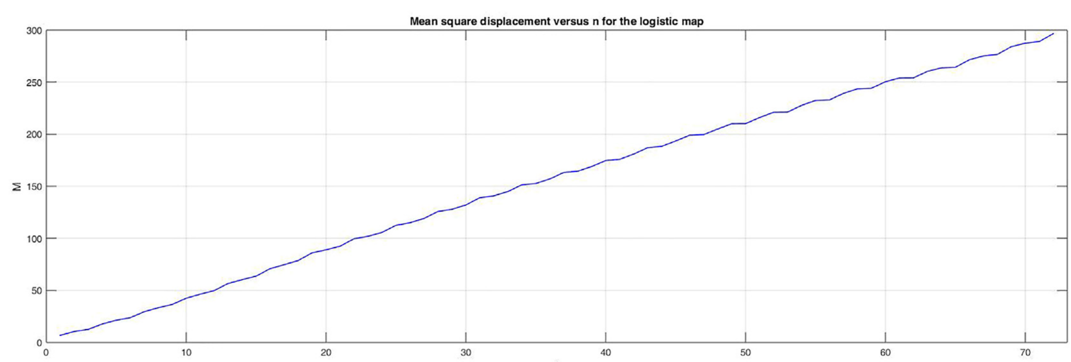

Fig. 7. The mean square displacement versus n for the logistic map.

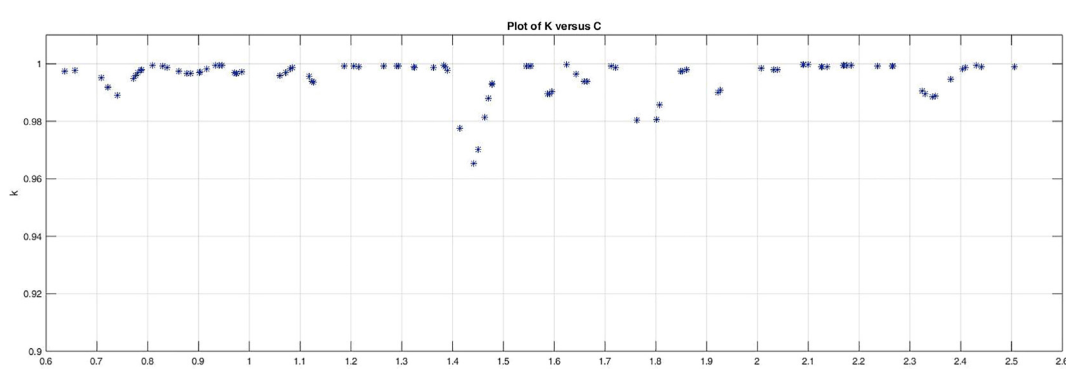

Fig. 8. The growth rate versus c.

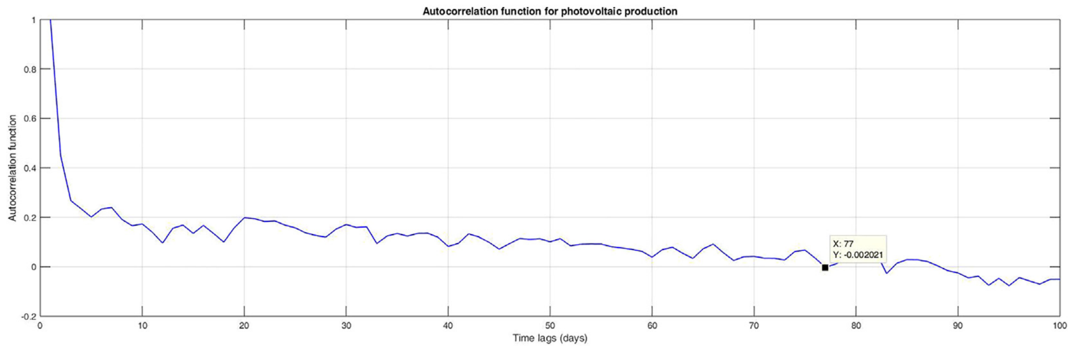

Fig. 9. Autocorrelation function for PV production.

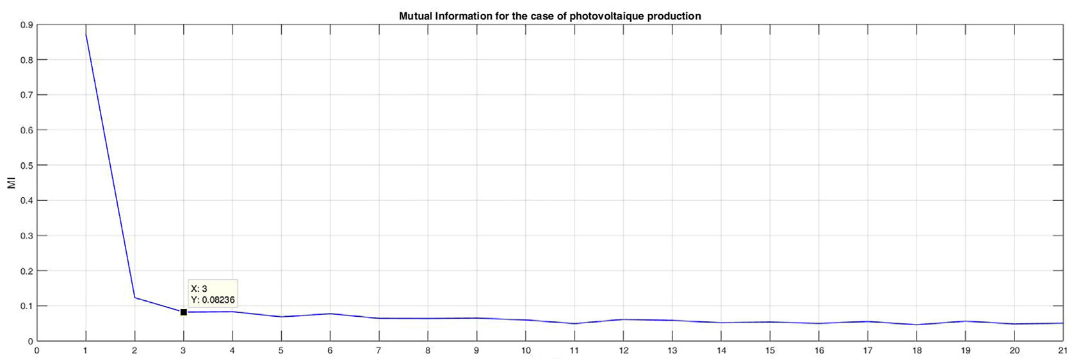

Fig. 10. Mutual information for the case of PV production.

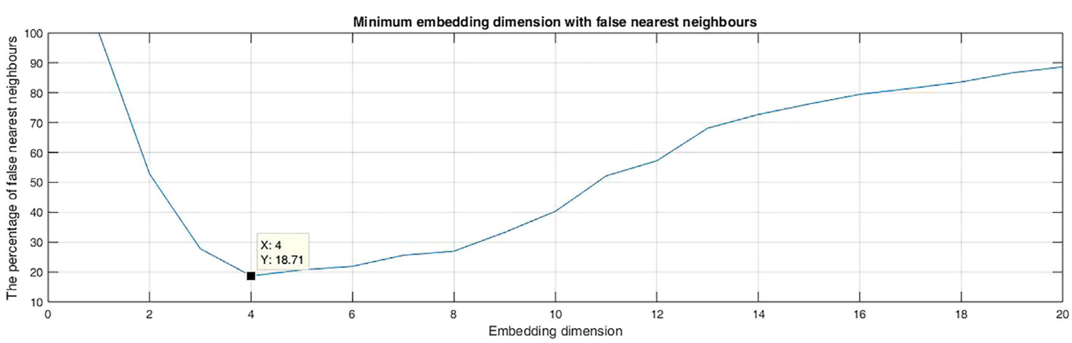

Fig. 11. Minimum embedding dimension with false nearest neighbors.

Fig. 13 shows the forecasts made by the ANN only, as well as those made with the ANNs after the reconstruction of the phase space compared to the real observations of the photovoltaic production. We note that the forecast after the phase space reconstruction is more efficient because of its responsiveness to peaks and fluctuation. The calculation of the mean squared error (MSE) presented in Table 1 confirm this conclusion. Where the MSE of the prediction with ANN is equal to 5.27723033 While after reconstruction of the phase space it becomes 5,06018. So a difference of 0,21705033. As for the regression coefficient, it increased from a value of 0.442618 for the forecast with ANN to a value of 0.49771233 after phase space reconstruction.

Fig. 14 shows the predictions made after phase space reconstruction with two methods, in the first, it is only the ANN, but in the second, ANN was associated with the wavelet transformation.

These forecasts are compared to real observations of photovoltaic production. We note that the prediction with the WRNN after reconstruction of the phase space is more efficient because of its reactivity to peaks and fluctuation. Which is confirmed by calculation of the mean squared error (MSE) given in Table 1. Where the MSE of the prediction with ANN after phase space reconstruction is equal to 5.06018 whereas with the WRNN after phase space reconstruction is 3.56337333. The difference of the error here is 1.49680667.

For the regression coefficient, it increased from a value of 0.49771233 for ANN prediction after phase space reconstructing to a value of 0.65975967 with WRNN after phase space reconstruction.

4. Conclusion and perspectives

The new approach for PV production forecasting that we propose in this work, is based on the exploitation of the phase space reconstruction, to build a database for the input of the neural

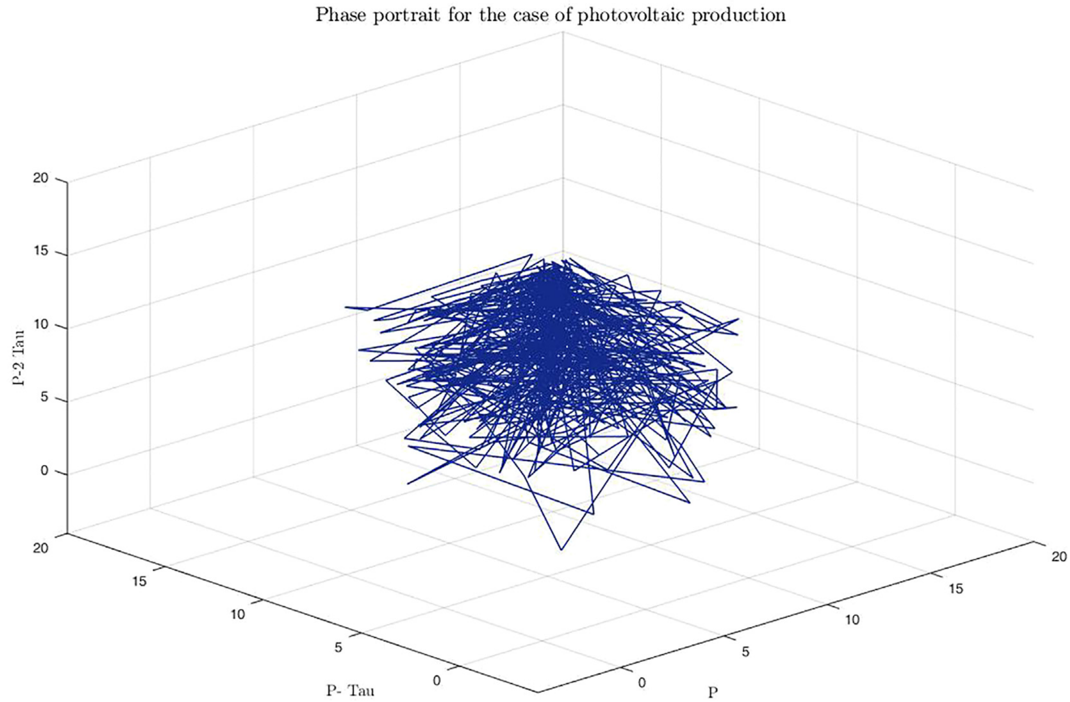

Fig. 12. Phase portrait for the case of photovoltaic production.

Table 1
The MSE for training, validation and testing.

MSE	ANN	ANN with phase space reconstruction	WRNN with phase space reconstruction
Training	5.07318 e−0	4.91908 e−0	3.63215 e−0
Validation	5.65801 e−0	5.68505 e−0	3.02671 e−0
Testing	5.100501 e−0	4.57641 e−0	4.03126 e−0

Table 2
The regression coefficient for training, validation and testing.

R	ANN	ANN with phase space reconstruction	WRNN with phase space reconstruction
Training	0,544404	0,573995	0,712635
Validation	0,393357	0,428486	0,625468
Testing	0,390093	0,490656	0,641176

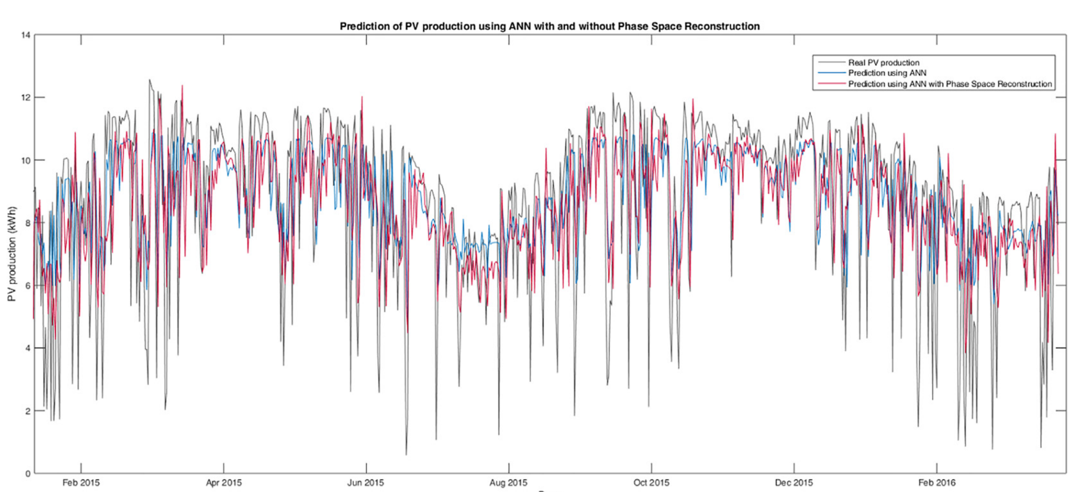

Fig. 13. Prediction of PV production using ANN with and without phase space reconstruction.

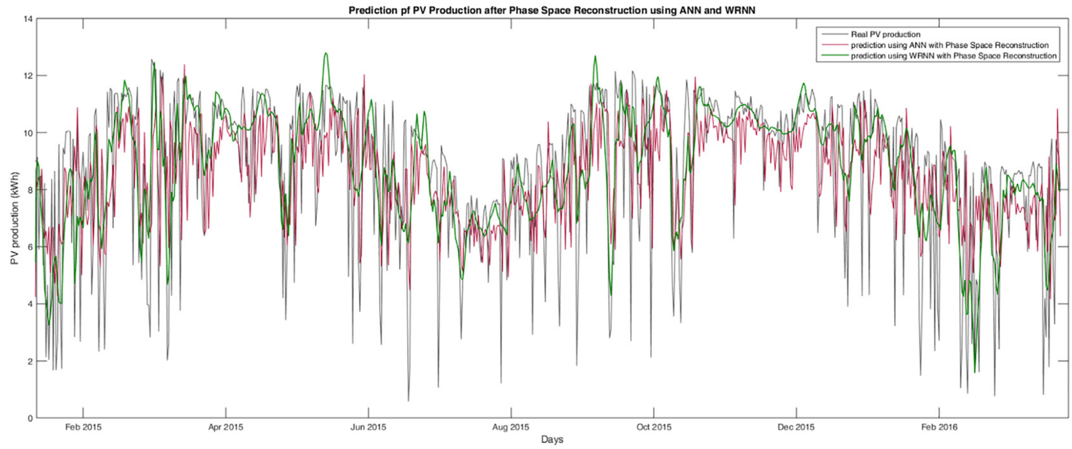

Fig. 14. Prediction of PV production after phase space reconstruction using ANN and WRNN.

network, so as to consider the system dynamics in the forecasting process. Then we have included the wavelet transformation to simplify the database constructed from phase space reconstruction in search of better precision. The comparison between the previsions and the real observations confirmed the efficiency of our approach. We could clearly enhance the forecasting results; however they cannot be described as perfect, given the chaotic character of photovoltaic energy. We concluded from this work that our system is confined to its strange attractor, certainly; but his movement on the attractor escapes us.

Therefore, we are unable to accurately determine the future of a chaotic system, such as photovoltaic energy, beyond a certain time. Since the notion of trajectory loses all meaning due to the sensitivity to the initial conditions. It is a question of proposing a deterministic model while leaving a space at random, a dimension to the unpredictable. It is a question of being interested in this tenuous margin which separates the mathematical zero from the almost nothing, the absolute accuracy of the best approximation. This margin slips between the mathematical model and the physical system that it is supposed to represent. Without forgetting the fact that, obviously, resort to a probabilistic approach is now necessary, including the notion of “events” that could be classified in a restricted number of possibilities.

Funding

This research received no external funding.

Conflicts of interest

The authors declare no conflict of interest.

Acknowledgments

This work exploits the data of photovoltaic panels installed as part of the Project "PROPRE.MA": sponsored by IRESEN from February 2014 for a period of 3 years, supported by 20 Moroccan institutions of higher education and a private company (RESING). The authors would like to thank IRESEN and all the partners as well as all those who contributed directly or indirectly to the realization of the project "PROPRE.MA".

References

[1] Poincaré, H., Le hasard, in Science Et méthode, B.d.p. Scientifique, Editor.: Paris. p. 64-95.
[2] E.N. Lorenz, Deterministic nonperiodic flow, J. Atmos. Sci. 20 (1963) 130–141.
[3] P.O. Vandervoort, On chaos in the pulsations of stars, Mon. Not. Roy. Astron. Soc. 443 (2014) 504–521.
[4] B.M. Garay, B.I., Chaos in Vallis' asymmetric Lorenz model for El Niño, Chaos, Solit. Fractals 75 (2015) 253–262.
[5] Y.W. Changjin Xu, Bifurcation and control of chaos in a chemical system, Appl. Math. Model. 39 (8) (2015) 2295–2310.
[6] J. van der Schaaf, J.R.v.O., F. Takens, J.C. Schouten, C.M. van den Bleek, Similarity between chaos analysis and frequency analysis of pressure fluctuations in fluidized beds, Chem. Eng. Sci. 59 (2004) 1829–1840.
[7] M.S. Nasir Ganikhodjaev, Ashraf Mohamed Nawi, Mutation and chaos in nonlinear models of heredity, Sci. World J. 2014 (2014), 835069, 11 pages.
[8] Tuan D. Pham, T.C.T. Mayumi Oyama-Higa, Masahide Sugiyama, Mental-disorder detection using chaos and nonlinear dynamical analysis of photoplethysmographic signals, Chaos, Solit. Fractals 51 (2013) 64–74.
[9] L.R. Irina Bashkirtseva, Tatyana Ryazanova, Stochastic sensitivity analysis of the variability of dynamics and transition to chaos in the business cycles model, Commun. Nonlinear Sci. Numer. Simulat. 54 (2018) (2017) 174–184.
[10] S. Lahmiri, On fractality and chaos in Moroccan family business stock returns and volatility, Physica A 473 (1 May 2017) 29–39.
[11] A.F.A. Saghafi, Global bifurcation and chaos analysis in nonlinear vibration of spur gear systems, Nonlinear Dynam. 75 (2014) 783–806.
[12] A. Guerine, A.E. H, L. Walha, T. Fakhfakh, M. Haddar, A polynomial chaos method for the analysis of the dynamic behavior of uncertain gear friction system, Eur. J. Mech.A Solids 59 (September–October 2016) 76–84.
[13] A.S.d.P. André Brandão, Marcelo Amorim Savi, Fabrice Thouverez, Nonlinear dynamics and chaos of a nonsmooth rotor-stator system, Math. Probl Eng. (2017).
[14] a, L.S. Jiang Wang, Xiangyang Fei, Bing Zhu, Chaos analysis of the electrical signal time series evoked by acupuncture, Chaos, Solit. Fractals 33 (2007) 901–907.
[15] B. Samardzic, B.M.Z., Analysis of spatial chaos appearance in cascade connected nonlinear electrical circuits, Chaos, Solit. Fractals 95 (2017) 14–20.
[16] U. Aich, Investigation for the presence of chaos in surface topography generated by EDM, Tribol. Int. 120 (April 2018) 411–433.
[17] B.S. Rahman Khatibi, Mohammad Ali Ghorbani, Ozgur Kisi, Kasim Koçak, Davod Farsadi Zadeh, Investigating chaos in river stage and discharge time series, J. Hydrol. 414 (415) (2011) 108–117.
[18] M.A.G. Manlio De Domenico, Oleg Makarynskyy, Dina Makarynska, Hakimeh Asadi, Chaos and reproduction in sea level, Appl. Math. Model. 37 (2013) 3687–3697.
[19] Reggie Brown, H.D.I.A. Paul Bryant, Computing the Lyapunov spectrum of a dynamical system from an observed time series, Phys. Rev. A 43 (6) (1991) 2787–2806.
[20] T. Michael, J.J.C.a.C.J.D.L. Rosenstein, A practical method for calculating largest Lyapunov exponents from small data sets, Physica D 65 (1993) 117–134.
[21] G.A.G.a.I. Melbourne, On the implementation of the 0–1, Test Chaos 8 (1) (2009) 129–145.
[22] L. Cao, Practical method for determining the minimum embedding dimension of a scalar time series, Physica D 110 (1997) 43–50.
[23] H.C.-z. MA Hong-guang, Selection of embedding dimension and delay time in phase space reconstruction, Front. Electr. Electron. Eng. China (2006) 111–114.
[24] M.M. Carl Rhodes, The false nearest neighbors algorithm: an overview, Comput. chem. Eng 21 (1997) 1149–1154.
[25] A.V. Kenya Andrésia de Oliveira, Elton Cesar da Silva, Using artificial neural networks to forecast chaotic time series, Physica A 284 (2000) 393–404.
[26] A.F. Fermín Rodríguez, Ainhoa Galarza, Luis Fontan, Predicting solar energy

generation through artificial neural networks using weather forecasts for microgrid control, Renew. Energy 126 (2018) (2018) 855–864.
[27] S.A. Kalogirou, E. M, V. Belessiotis, Artificial neural networks for the performance prediction of large solar systems, Renew. Energy 63 (2014) (2014) 90–97.
[28] G.N. Cyril Voyant, Soteris Kalogirou, Marie-Laure Nivet, Christophe Paoli, Fabrice Motte, Alexis Fouilloy, Machine learning methods for solar radiation forecasting: a review, Renew. Energy 105 (2017) (2017) 569e582.
[29] M. Carolin Mabel, E.F, Analysis of wind power generation and prediction using ANN: a case study, Renew. Energy 33 (2008) (2007) 986–992.
[30] P. Ramasamy, S.S. C, Amit Kumar Yadav, Wind speed prediction in the mountainous region of India using an artificial neural network model, Renew. Energy 80 (2015) (2015) 338–347.
[31] T.C. McCandless, S.E.H, G.S. Young, A regime-dependent artificial neural network technique for short- range solar irradiance forecasting, Renew. Energy 89 (2016) (2015) 351–359.
[32] J.W. Lili Huang, Forecasting energy fluctuation model by wavelet decomposition and stochastic recurrent wavelet neural network, Neurocomputing 309 (2018) (2018) 70–82.
[33] J.P.S. Catalão, H.M.I.P, V.M.F. Mendes, Short-term wind power forecasting in Portugal by neural networks and wavelet transform, Renew. Energy 36 (2011) (2011) 1245–1251.
[34] D.Y. Vishal Sharma, Wilfred Walsh, Thomas Reindl, Short term solar irradiance forecasting using a mixed wavelet neural network, Renew. Energy 90 (2016) (2016) 481–492.
[35] C.V. Madasthu Santhosh, D.M. Vinod Kumar, Ensemble empirical mode decomposition based adaptive wavelet neural network method for wind speed prediction, Energy Convers. Manag. 168 (2018) (2018) 482–493.